Chapter 5
Lander/Cu(111) – Molecule-Metal Contact

In a single molecule device, made of a molecule connected to metallic electrodes, the electronic contact of the molecule with its metal electrodes plays a fundamental role.[2] Recent investigations have shown that the contact resistance depends on many parameters[14, 123], which are often difficult to control, and relies on the precise interaction between the molecular end groups and the surface of each electrode[16, 17]. The characteristics of a hybrid electronic contact can be clearly understood when the edges of the electrodes are atomically ordered, clean, and when the geometry of the molecule at the junction is under control at the atomic scale (see Eq. (3-1)). Abandoning atomically clean contact conditions leads to characteristics randomly changing from device to device[14, 18], with the consequent large increase of the number of molecules per device necessary to stabilize its electronic functions[123]. By means of break-junction experiments, measurements of current-voltage (I-V) characteristics on single molecules have been recently reported.[12, 13] In break-junctions a micro-fabricated electrode is gently fractured by mechanical deformation while measuring the resistance of the junction.[124] Molecules are injected in the junction by means of a liquid evaporation step. However, the application to single molecules is difficult, since the exact number of interconnected molecules, the exact conformation of the molecule, and the exact geometry of the metal electrodes remain essentially inaccessible.[13] Theoretical works have predicted a strong variation of I-V characteristics due to the

atomic structure of the contact region between molecule and electrode[18, 125], as could also be confirmed by means of break-junction experiments[15].

This work reports on the first detailed investigation of an atomically defined contact between a molecular wire and a metal contact pad. This was the initial aim of the synthesis of the Lander molecule (see section 3.3.1 for a description of the molecule).[16, 91] The idea is to contact a Lander molecule with the end part of the molecular wire board to a metallic step edge, as a model of an atomically defined electrode. Standing wave patterns from surface state electrons will be used to observe the local electronic perturbation caused by the interaction between the molecular wire end and the metallic mono-atomic step edge.

Moreover, the properties of the Lander molecule as a scatterer of the surface state electrons are investigated in detail. It is known that on metal surfaces exhibiting Shockley-type surface states[84], defects such as adsorbed atoms[88], rows of adatoms[126], and step edges[127] act as scattering centres for the surface state electrons. The resulting surface standing wave patterns in the LDOS can be observed by LT-STM. On the Cu(111) surface, when operating the STM at low bias voltages ($|V| < 100$ mV), these oscillations become visible with a wavelength of about 15 Å equivalent to $\lambda_{Fermi}/2$. At higher tunnelling voltages ($E > 250$ meV) oscillations are not exactly visible since surface states with different wavelength superimpose. However, using the technique of dI/dV mapping, the standing wave patterns of surface state electrons can be measured as a function of energy.

In the case of a Lander molecule on Cu(111), the size of the scattering object is in the order of the surface state wavelength. Therefore the scatterer will not behave point like and the internal structure of the molecule will influence the standing wave patterns. I will show that, for large organic molecules, the surface waves become a very useful tool to reveal the weak interactions of different parts of the molecule with the surface. Such information is important for the development of single molecular devices but hardly accessible to STM otherwise. In this context, an important example is the study of a metal-molecule-metal bridge in the group of Ho[128], where a single phthalocyanine molecule has been positioned between two chains of gold adatoms.

5.1 Adsorption Geometry

When Lander or Reactive Lander molecules are sublimated on a Cu(111) substrate maintained at room temperature, they align themselves along the edge of the mono-atomic steps with two legs on the upper terrace and the two others on the lower terrace. Their board is parallel to the step and located on the upper terrace (Fig. 5.1). This conformation is comparable to the one observed along the mono-atomic steps of the Cu(100) surface (Fig. 3.9).[93]

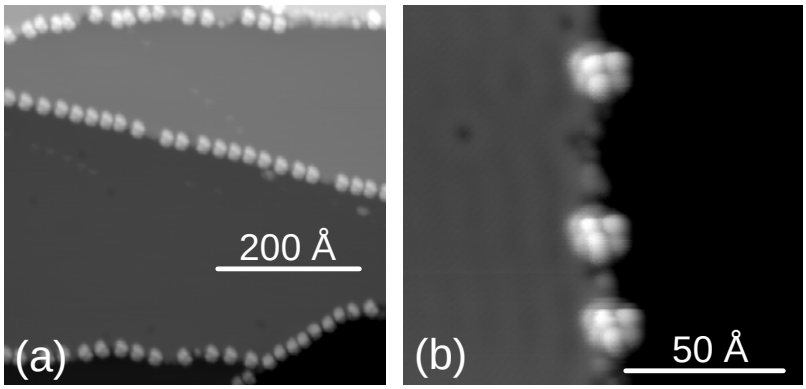

Fig. 5.1. STM measurements after preparation of Lander molecules on Cu(111) at 320 K sample temperature. (a) U = 1.0 V, I = 0.2 nA. (b) U = 0.1V, I = 0.1 nA.

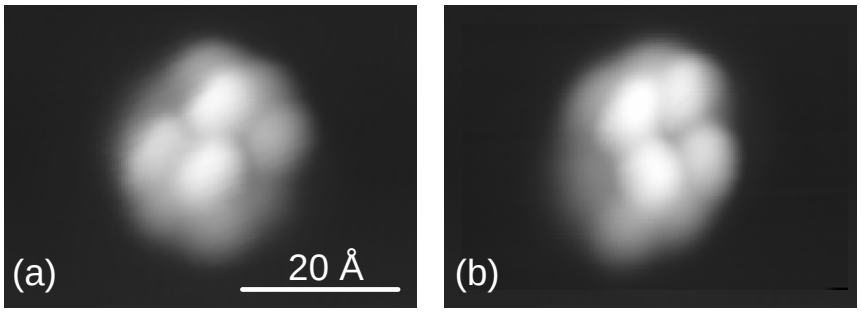

Fig. 5.2. STM measurements of Lander molecules on Cu(111) (I = 0.2 nA, U = 0.8 V). (a) Crossed legs conformations. (b) Parallel legs conformation.

On the contrary, when the Lander molecules are sublimed while keeping the substrate at a temperature of 20 K, they are found isolated on the Cu(111) terraces as shown in Fig. 5.2. Again molecules are found in the known conformations, i.e.

crossed legs and parallel legs as observed on Cu(211) (see section 4.1), Cu (100)[93] and Cu (110)[95, 96]. As in the previously described cases, only the molecular TBP legs are imaged in STM measurements. From MM+ESQC calculations it is known that the average board height on Cu(111) is 3.6 Å.

5.2 Manipulation

Lander molecules can be laterally manipulated by means STM by employing the constant height manipulation mode. In Fig. 5.3 a SL molecule prior (a) and after (b) the performance of an STM induced manipulation is shown. When Lander molecules are manipulated on Cu(111) their conformation and their orientation change in most cases (contrary to manipulation along the step edges on Cu(211)). The typical signal, which is obtained when a SL molecule is laterally manipulated in constant height mode is shown in Fig. 5.3(c).

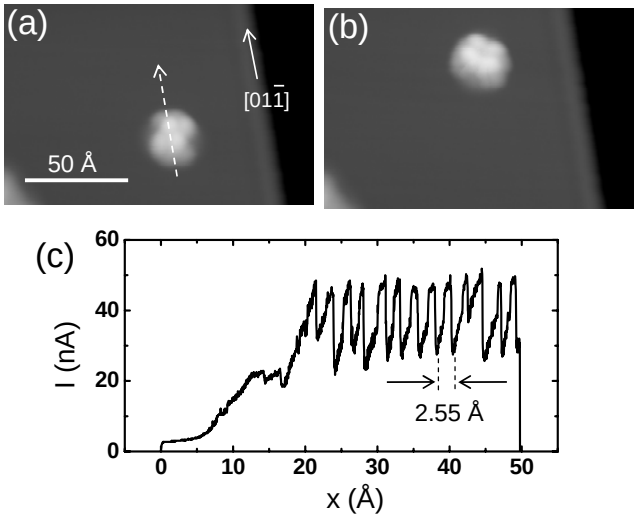

Fig. 5.3. Constant height manipulation of a SL molecule on Cu(111) along the close-packed direction. (a) STM image before manipulation, with the movement path of the tip during manipulation indicated and (b) STM image after manipulation. The manipulation signal (c) shows the typical saw-tooth signal for manipulation in pushing mode, the periodicity of 2.55 Å corresponds to the substrate lattice.

In this case the molecule is moved parallel to the close-packed direction of the sample, hence the manipulation signal has the form of a saw-tooth, typical for pushing, with the periodicity of 2.55 Å, the nearest neighbour distance of Cu(111). Beside the regular saw-tooth the signal shows no internal structure. This observation is in contrast to an other molecule with TBP legs: Cu-tetra-3,5 di-*tert*-butyl-phenyl porphyrin (TBPP), which has recently been investigated by Moresco et al.[54, 55] In the case of TBPP the contribution of each single leg leads to a characteristic signature in the tunnelling current. Therefore several local minima and maxima show up within each period (of 2.55 Å length), allowing the calculation of the individual movement of each leg.[54] In the present case the signal seems only determined by the corrugation of the substrate. However, the contribution to such signals due to the legs and to the board can be distinguished by MM+ESQC calculations as recently shown for Lander on Cu(211) by Alemani et al.[122]

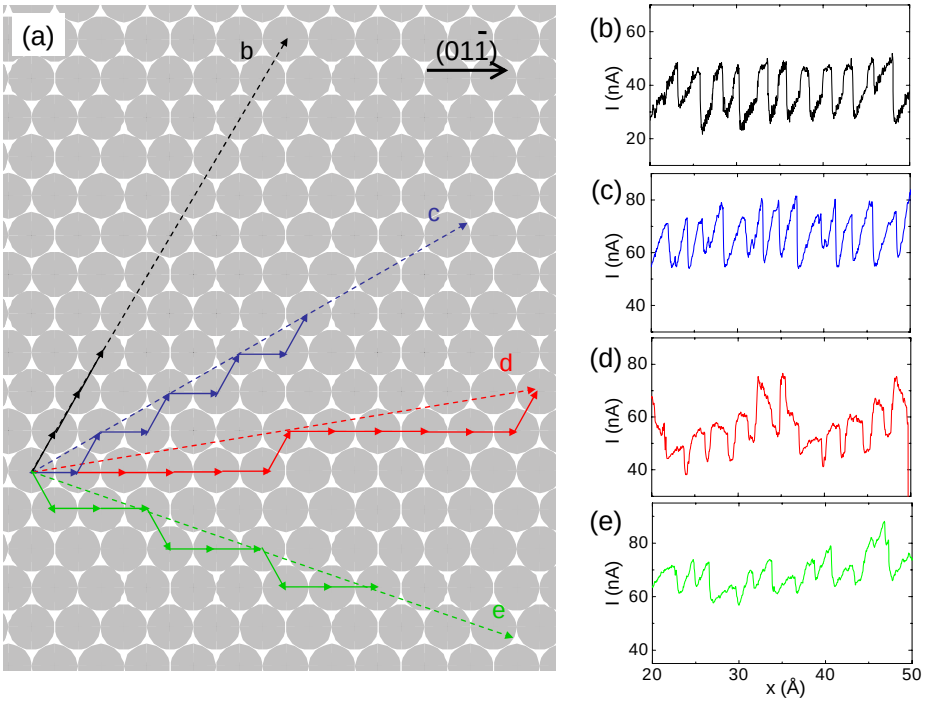

Fig. 5.4. (a) Schematic model for the manipulation of Lander molecules in different directions with respect to the substrate $[01\bar{1}]$ direction. The dashed arrows indicate the path of the STM tip, while the solid arrows of 2.55 Å length indicate the atomic hops of the molecule. The manipulation signals are shown for manipulation inclined by 0° (b), 30° (c), 10° (d), and 20° (e) with respect to the $[01\bar{1}]$ direction.

In cases where the manipulation direction is not parallel to a close-packed direction of the sample, the manipulation signal can be explained by atomic jumps along two different close-packed directions in a periodical manner (Fig. 5.4(a)), similar to the observations of Hla et al. on manipulation experiments with single atoms.[129]

If the manipulation direction is exactly tilted 30° with respect to a close-packed direction as in Fig. 5.4(c), i.e. exactly bisecting the angle between two close-packed directions, the molecule makes alternating jumps of 2.55 Å length along the two close-packed directions. Since the angle between molecular movement and tip movement is 30° for each jump, the recorded manipulation signal shows a periodicity of (2.55Å × cos(30°)) = 2.21 Å. For a manipulation direction, which is only a few degrees tilted from a close-packed direction, the molecule moves several atomic jumps in that close-packed direction and then one atomic jump to the next parallel close-packed line of atoms. This results in a manipulation signal as shown in Fig. 5.4(d). In this case, the manipulation is tilted by 10° with respect to the $[01\bar{1}]$ direction, resulting in a periodicity of six atomic jumps, explained by 5 jumps in $[01\bar{1}]$ direction, followed by one jump to the next line of close-packed atoms. When the manipulation direction is tilted by 20° with respect to the $[01\bar{1}]$ direction, the molecule jumps two steps in $[01\bar{1}]$ direction and every third step in the direction of 60°, as can be deduced from the manipulation signal as shown in Fig. 5.4(e).

From the observed manipulation signals, it follows that the molecule always hops in steps of a distance of a = 2.55 Å in the direction of one of the close-packed directions of the substrate. Thus, the molecule adsorbs at only one defined adsorption site within the substrate unit cell during the manipulation. This is a remarkably observation for such a large molecule covering an area of approximately 50 surface atoms. The problem is however to address the tunnelling signal to a specific part of the molecule and to determine the preferred adsorption site.

In a recent investigation we analyse the manipulation of SL on Cu(211) using MM+ESQC calculations.[122] The manipulation curves on Cu(211) are qualitatively

identical to those on Cu(111), when comparing manipulation in $[01\bar{1}]$ direction. Therefore the description for the (211) surface will hold also in case of the (111) surface qualitatively, at least for manipulation in $[01\bar{1}]$ direction. The saw-tooth signal, observed for manipulation in $[01\bar{1}]$ direction on Cu(211) and Cu(111), is explained as follows: During the manipulation process the tunnelling current contributing from the molecular board dramatically increases, due to the reduced tip height and a further reduced board-surface distance. For this reason the signature in the manipulation experiments mainly results from tunnelling trough the molecular board, thus explaining why no features, arising from rotational deformation of the molecular legs, are visible in the manipulation signal. The board hops from one stable adsorption site to the next, giving rise to the typical saw-tooth signal with the substrate periodicity. The legs will tilt during the manipulation, but their influence on the manipulation signal is negligible.

5.3 Scattering of Surface State Electrons at Lander Molecules

A topographic STM image of a RL molecule (Fig. 5.5 (a)) shows the same geometry as the well-studied SL[93, 95-98]. As has been already shown for the SL, the visible lobes correspond to the four di-*tert*-butyl-phenyl groups (legs) of the molecule, while the molecular board is not visible in STM topographs on a flat surface. As already discussed, two different conformations, i.e. parallel legs and crossed legs, are observed. The same conformations are obtained for the RL and similar conformations of RL molecules have also been observed on Cu(110).[63] Moreover, SL and RL are not distinguishable by their appearance in STM topographs, since the position of the legs along the board is identical for both molecules. By comparing STM measurements with MM+ESQC calculations, the orientation of the molecular board and the conformation of the spacer legs can be determined.[93, 95] Conformation and orientation of the molecule in Fig. 5.6 are deduced from the constant current image in Fig. 5.6(a). The molecule shows the

crossed legs conformation and the board in this case is rotated by about 19° clockwise with respect to the horizontal line as shown in the model in Fig. 5.6(b).

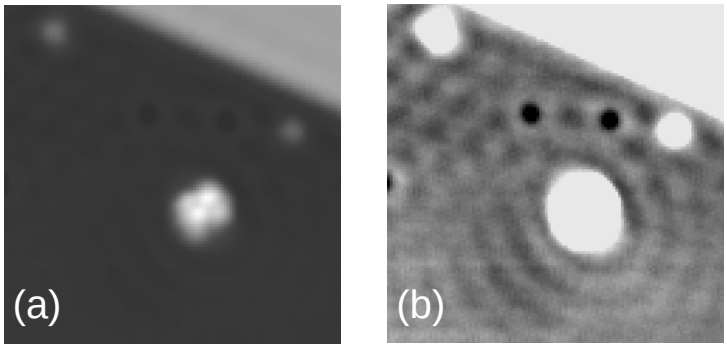

Fig. 5.5. Reactive Lander on a Cu(111) terrace, images (a) and (b) show the same measurement (U = 100 mV; I = 0.3 nA; size: 15×15 nm²) with different contrast. From comparison of (a) with ESQC calculations the orientation of the board can be deduced, (b) shows the standing wave patterns obtained with constant current, which are always in an elliptical shape, with the long axis parallel to the molecular board.

dI/dV maps of the same RL molecule were recorded at different voltages (Fig. 5.6 (c)-(e)). The standing wave patterns are clearly visible in the dI/dV maps. They are of an oval shape with the long axis parallel to the molecular board. According to the parabolic dispersion relation, the wavelength decreases with increasing energy from the surface state energy onset (E_Γ = -420 meV). The dispersion is in good approximation free electron like for energies smaller than 2 eV with an effective mass of $m^* = 0.40\ m_e$.[89] The dI/dV maps are recorded in constant current mode because of the large apparent height of the molecule (4.0 Å). This means that the feedback loop remains enabled with a time constant that is fast enough to follow the topology of the surface (scan speed is in the order of a few sec/line) but too slow to follow the modulation amplitude (typically ν = 380 Hz). Topography (Fig. 5.6(a)) and dI/dV map (Fig. 5.6(e)) at the same bias voltage are measured simultaneously in this mode.

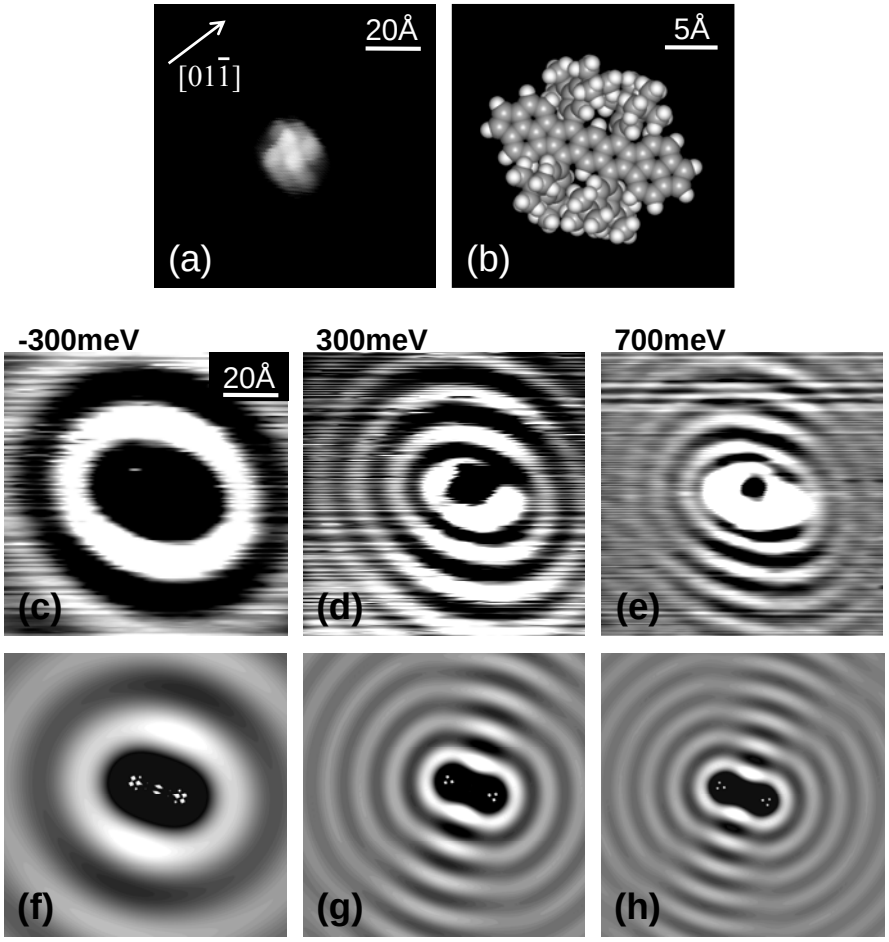

Fig. 5.6. RL molecule on a Cu(111) terrace. All measurements (a),(c-e) show the same surface area (10×10 nm²). From the constant current STM measurement (a) (U = 700 mV, I = 0.2 nA) the orientation and conformation of the molecule can be deduced, as shown in the model (b). Standing wave patterns are measured by means of dI/dV maps (c), (d), and (e) recorded at V_{bias} = -300 meV, 300 meV, and 700 meV, respectively. The same voltage was both used to set the height of the tip (with I = 0.2 nA) and to measure dI/dV at V_{bias}. (f)-(h) Multiple scattering calculations (see text), corresponding to the bias voltages of (c)-(e), respectively.

To understand how the different parts of the RL molecule contribute to the scattering of the surface state electrons, I reproduce the geometry of the RL scattering pattern using multiple scattering calculations. To calculate STM images of the surface state wave patterns, a technique from E. J. Heller et al.[88] is adopted, which initially was used to describe the scattering patterns inside quantum corrals, as shown in Fig. 2.3.

Heller models the electron amplitude emitted by the tip at distance *r* by a cylindrical wave, which in the limit of large *kr* is:

$$a_T(r) = \sqrt{\frac{2}{\pi k}} \frac{e^{ikr - i\pi/4}}{\sqrt{r}}, \tag{5-1}$$

where the wave number *k* is given by the dispersion relation. The dispersion relation is assumed to be free-electron like, i.e.

$$k(E) = \sqrt{\frac{2m^*(E - E_\Gamma)}{\hbar^2}}, \tag{5-2}$$

with the effective mass m^* and the onset of the band-edge energy E_Γ. The amplitude of the wave that is emitted by the tip and scattered once at a scatterer (labelled *j*) at distance r_j is

$$a_T(r_j)a(r) = a_T(r_j)\sqrt{\frac{2}{\pi k}} \frac{e^{ikr}}{\sqrt{r}} e^{i\pi/4} \frac{(\alpha_0 e^{2i\delta_0} - 1)}{2i}, \tag{5-3}$$

In this case α_0 and δ_0 are the parameters characterising the scatterer, both are real numbers, with $\alpha_0 \in [0,1]$ and $\delta_0 \in [-\pi, \pi]$ is the scattering phase shift. In the original work of Heller one complex scattering parameter η_0 or a_0 is used instead of α_0 and δ_0 with

$$\frac{\left(\alpha_0 e^{2i\delta_0} - 1\right)}{2i} = \frac{\left(e^{2i\eta_0} - 1\right)}{2i} = a_0 . \tag{5-4}$$

The important case of a so called black dot scatterer is reached in the black dot limit, which corresponds to

$$\mathrm{Im}(\eta_0) \to \infty, \tag{5-5}$$

or equivalently to $a_0 = \frac{i}{2}$ or $\alpha_0 = 0$ independent of δ_0.

The total amplitude $g_1(r)$ for scattering once and returning to the tip at r is

$$g_1(r) = \sum_j a_T(r_j)\, a(r_j)\,, \tag{5-6}$$

The interference term is

$$I(r,k) = 2\,\mathrm{Re}\left[g_1(r)\right]\ , \tag{5-7}$$

which can also be written in matrix notation

$$I(r,k) = 2\,\mathrm{Re}\left[\vec{a}_T(r)\cdot\vec{a}(r)\right]\ , \tag{5-8}$$

$$\text{with}\ \ \vec{a}_T(r) = \begin{pmatrix} a_T(r_1) \\ \ldots \\ a_T(r_N) \end{pmatrix}\ \ \text{and}\ \ \vec{a}(r) = \begin{pmatrix} a_1(r_1) \\ \ldots \\ a_N(r_N) \end{pmatrix}. \tag{5-9}$$

To treat multiple scattering the scattering matrix A_{ij} is introduced. When summing up all possible numbers of scattering processes one obtains the series

$$I(r,k) = 2\,\mathrm{Re}\left[\vec{a}_T(r)\cdot\vec{a}(r) + \vec{a}_T(r)\cdot A\cdot\vec{a}(r) + \vec{a}_T(r)\cdot A^2\cdot\vec{a}(r) + \ldots\right] \tag{5-10}$$

$$\text{with}\quad \begin{array}{ll} A_{ij} = a_i(r_j) & for\ \ i \neq j \\ A_{ij} = 0 & for\ \ i = j \end{array} \tag{5-11}$$

Note that the scattering matrix A is independent of r, which means A has only to be calculated once for a given scattering geometry and energy. If the series in (5-10) converges the limit is

$$I(r,k) = 2\,\mathrm{Re}\left[\vec{a}_T(r)\cdot(1-A^{-1})\cdot\vec{a}(r)\right]. \tag{5-12}$$

Using this formula, STM images of standing wave patters of a known geometry of point-like scatterers can be simulated. Within this work a Fortran program was written to calculate standing wave patterns dependent on the surface state wavelength, the position of scatterers, the scattering phase shift, and scattering amplitude of scatterers. For a more detailed description of multiple scattering calculations see [130-132].

Inside the Lander molecule two qualitatively different parts can be distinguished, which therefore might behave as unequal scatterers of the surface state electrons. On one hand the TBP legs, consisting of sp^3 carbon atoms, beside one central phenyl ring per leg, rotated by about 42° out of the surface plane; on the other hand the molecular board, an aromatic π-system parallel to the surface and maintained elevated 0.1 nm away from the chemisorption distance to the surface, which would be obtained without the spacer legs. The exact rotation of the molecular legs and the elevation of the molecular board are extracted from the adsorption geometry and conformation that have been determined with molecular mechanics calculations and were confirmed by comparison of calculated STM images (using ESQC) with experimental data.

For simplicity I assume that the positions of the scatterers correspond to the positions of the carbon atoms of the molecule. In all simulations it is assumed that the scatterers act as ideal black dots, i.e. they have an absorption coefficient of 1. It has been found that the black dot limit[88] is a good approximation for simulating the positions of maxima and minima in standing wave patterns. The standing wave patterns for different energies are calculated using the dispersion relation for surface state electrons on Cu(111).[89]

The wave patterns produced by a RL molecule have been calculated for three different model geometries (Fig. 5.7). The first one (see model Fig. 5.7(a)) corresponds to scattering centres at the position of the board only, the second (Fig. 5.7(b)) to scattering centres at legs and board, the third (Fig. 5.7(c)) takes into account only the legs. To model the legs (b, c), I consider the scatterers only at the atom positions corresponding to the aromatic ring of the legs, neglecting the butyl groups.

The interpretation of the dI/dV maps recorded in constant current mode as LDOS is not straightforward and is in principle allowed only if the tip is scanning in constant height.[133] As the experiments are performed in constant current mode, we have to exclude the points corresponding to the molecule and in its vicinity (up to 7 Å) because of the changes in tip height. Also dI/dV maps at small tunnelling voltages (-250 mV to +250 mV), at which the tip height itself is

significantly affected by standing wave patterns, should be excluded from the comparison with the calculations. Using dI/dV mapping in constant current mode standing wave patterns for the RL molecule from 300 meV to 1000 meV and at -300 meV are measured. By using STM topographs at small energies (< 100 meV) the standing wave patterns at the Fermi energy are recorded.

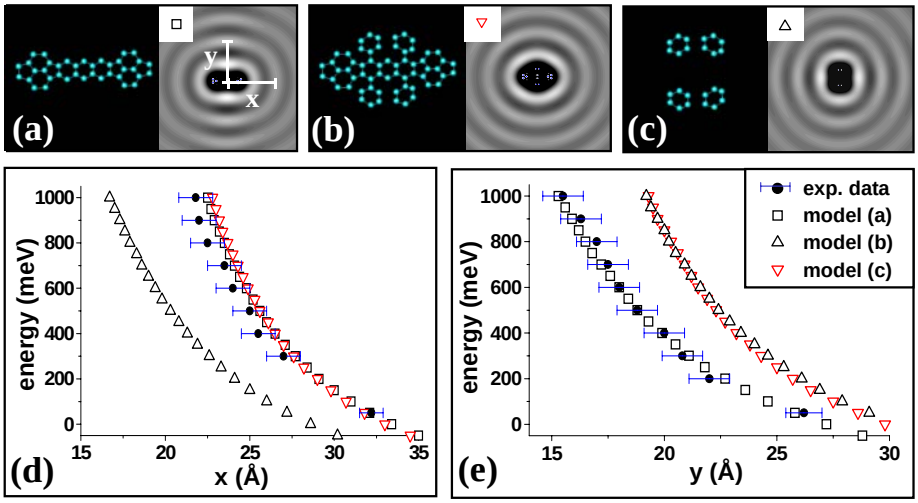

Fig. 5.7. Model calculations for the standing wave patterns of a RL molecule. Models (a)-(c) show the position of scattering centres (left) and corresponding multiple scattering calculations at E = 0 meV (right) (9×9 nm²). Model (a) is taking into account scattering of only the molecular board, (b) scattering of board and legs, and (c) scattering of legs only. In graphs (d), ((e)) the distance *x* (*y*) of the second maximum from the molecular centre parallel (perpendicular) to the molecular board is plotted as a function of energy.

The multiple scattering calculations are compared with the experimental data for the three geometries already described, by measuring the distance of the second standing wave maximum to the molecular centre. The distance measured parallel to the molecular board is called *x* and the distance measured perpendicular to it is called *y*, as sketched in Fig. 3(a). The position of the second maximum is sufficiently distant to ensure no tunnelling through the molecule, but near enough to reveal the specific geometry of the scatterer.

As one can see in Fig. 5.7(d) and (e), only the model shown in Fig. 5.7(a) leads to

a good agreement with the experimental data for both *x* and *y*. Scattering from only the legs (model (c)) yields the worst agreement between the three models, as in this case the distance *x* is even smaller than *y*, in contradiction to the experimental results. Model (b) succeeds in reproducing the correct length for *x*, but the value for *y* is overestimated. On the other hand, the calculation for model (a) reproduces well the oval shape of the standing wave patterns for all measured energies (-300 meV, 0 eV and energies from 300 meV to 1000 meV) with the correct values for *x* and *y*. Some examples of multi-scattering calculations obtained with this model for different energies are shown in Fig. 5.6(f)-(h).

Since the calculations indicate a dominant role of the board in the scattering of the surface state electrons, changes in the board length should be reflected in the standing wave patterns. To confirm this point the standing wave patterns of the three Lander type molecules, as shown in Fig. 5.7 (SL, RL, and VL), are compared.

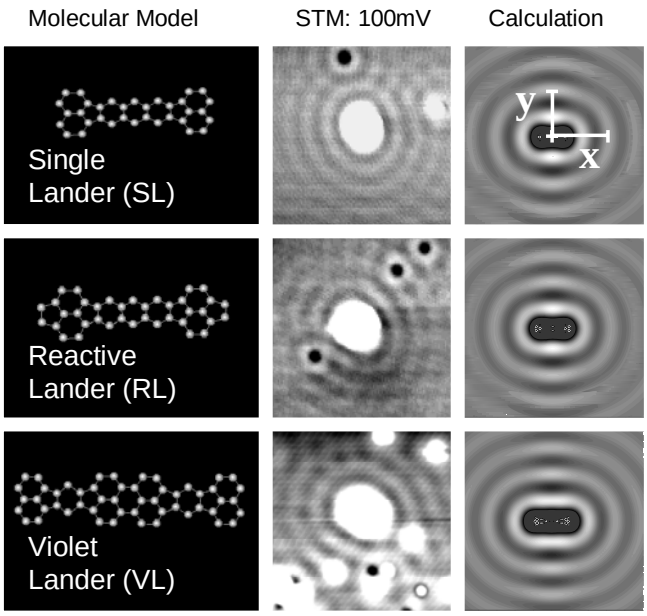

Fig. 5.8. Standing wave patterns of SL, RL, and VL. Models of the molecular board are shown in the left panel, typical STM measurements in the central panel (V = 100 mV, I = 0.1 nA, 11×11 nm²), and calculations of standing wave patterns (9×9 nm²) in the right panel. For the calculations scattering centres in the geometry of the molecular board have been employed.

Molecule	Axis	Experimental (Å)	Scattering calculation (Å)
Single Lander (SL)	X	30.0 ± 1.2	31.2
	Y	25.5 ± 1.0	26.0
Reactive Lander (RL)	X	32.2 ± 0.8	32.1
	Y	26.2 ± 0.7	25.9
Violet Lander (VL)	X	33.2 ± 2.9	34.7
	Y	26.0 ± 2.0	26.0

Table 5.1. Comparison of measured values for *x* and *y* for the different Lander type molecules near the Fermi level (E = 50 meV) using multiple scattering calculations, taking into account only scattering of the molecular board.

Measured and calculated values for *x* and *y* near the Fermi level (E = 50 meV) for the three different molecules are listed in Table 5.1. Each experimental value is averaged over at least 20 STM measurements of different molecules, typical measurements are shown in Fig. 5.8. The error in the axis length for the VL molecule is rather large because we did not obtain a clean preparation for this molecule, since the evaporation temperature of the molecule is to large to ensure evaporation without fragmentation. The calculations for the different molecules are taking into account scattering from only the board, as shown in models in Fig. 5.7. While along the axis perpendicular to the board (*y*) the same values for all three molecules are obtained, the different lengths of the molecular board influence the length *x*, which increases with increasing length of the molecule. This result confirms the strong influence of the molecular board on the standing wave pattern. For Lander molecules adsorbed on Cu(111), it can then be concluded that the molecular board is responsible for the observed surface state scattering and that the legs are only very weak scatterers. The reason for the weak scattering at the molecular legs is presumably that on the one hand each leg chemical groups close to the surface are hydrogen saturated carbons (TBP groups) and on the other hand that the central phenyl ring of each leg is rotated by about 42°, an unfavourable orientation for its π molecular orbitals to polarize the surface electrons.

Despite the fact that by design the spacer legs are elevating the molecular board away from the Cu(111) surface, there is still an electronic interaction between the π molecular orbitals of the Lander board and surface states. This interaction is not strong enough to permit the board to show up in a standard STM image but active enough to build up a scattering centre for surface electrons. This confirms other observations about the adsorption of Lander molecules: It is known that the interaction of the Lander molecular board with the surface forces the legs of the Lander to rotate and deform, allowing a smaller board surface separation than anticipated for a rigid molecule model, as has been shown in the previous chapter (section 4.2). Moreover, surface restructuring due to the presence of Lander molecules has been observed and the interaction between board and surface has been addressed as driving force for these restructurings.[95, 98]

5.4 Contacting Lander Molecules to Step Edges

To mimic the contact edge of an atomically ordered electrode, dislocation steps on a Cu(111) surface are fabricated. The stable and extremely clean mono-atomic steps (0.209 nm in height) required for the molecule-step edge contact experiments are created by a controlled crash of the tip into the surface, thus forming several hundred nm long dislocation steps with mono-atomic height. The tip is indented several 10 nm into the substrate thereby creating dislocations and causing gliding along the preferred <110> slip systems (see section 3.2.1). After the step formation, the tip is moved laterally away from the crashing zone to find an atomically clean surface area in spite of the presence of dislocation steps.

Fig. 5.9(a) shows an artificial step edge (running from left to right) and a natural step edge (running vertically). The natural step exhibits many defects and kinks and is covered with adsorbates since it was existing during the preparation already. In this case the sample was at room temperature, therefore the Lander molecules are adsorbed at step edges. The artificial step, which was created by a

tip crash, is straight with a very low density of defects and kinks. By means of lateral STM manipulation a Lander molecule can be brought close to a step edge, as is shown in Fig. 5.9(b).

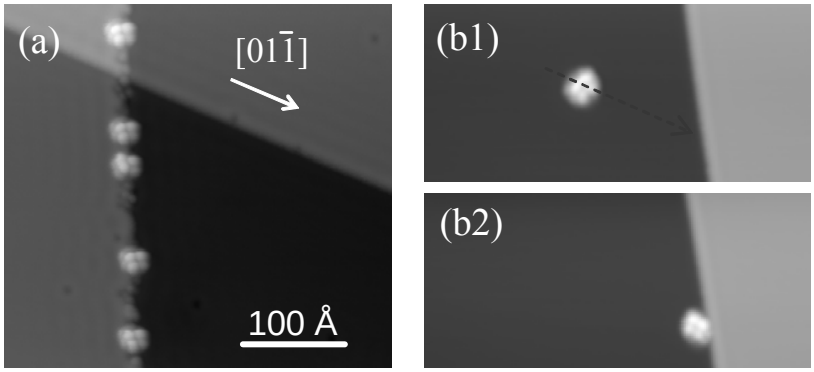

Fig. 5.9. (a) Comparison of a natural step (vertical) and an artificial step (horizontal), which has been induced by a controlled tip crash several 100 nm away from the shown region. Preparation was at room temperature in this case, therefore Lander molecules are adsorbed at natural step edges. A Lander molecule (b1) can be brought close to artificial step edges by STM manipulation (b2).

The panel in Fig. 5.10 shows Lander molecules at different adsorption sites with respect to a dislocation step edge. Fig. 5.10 A3 shows a typical STM image of a single isolated Lander on a terrace. Its conformation was identified by combining the STM-ESQC image calculation technique with a molecular mechanics optimization of the molecular geometry on the surface, allowing each calculated STM constant current scan to converge towards the experimental one.[99] As described in detail in the previous section (5.3) a Lander molecule, adsorbed on a clean Cu(111) terrace acts as a scattering centre for the corresponding 2D electronic states and creates an oval standing wave pattern as visible in Fig. 5.10 A4. The standing wave patterns due to the fabricated step edge are also observed in the same conditions on the upper terrace (see Fig. 5.10 B4).

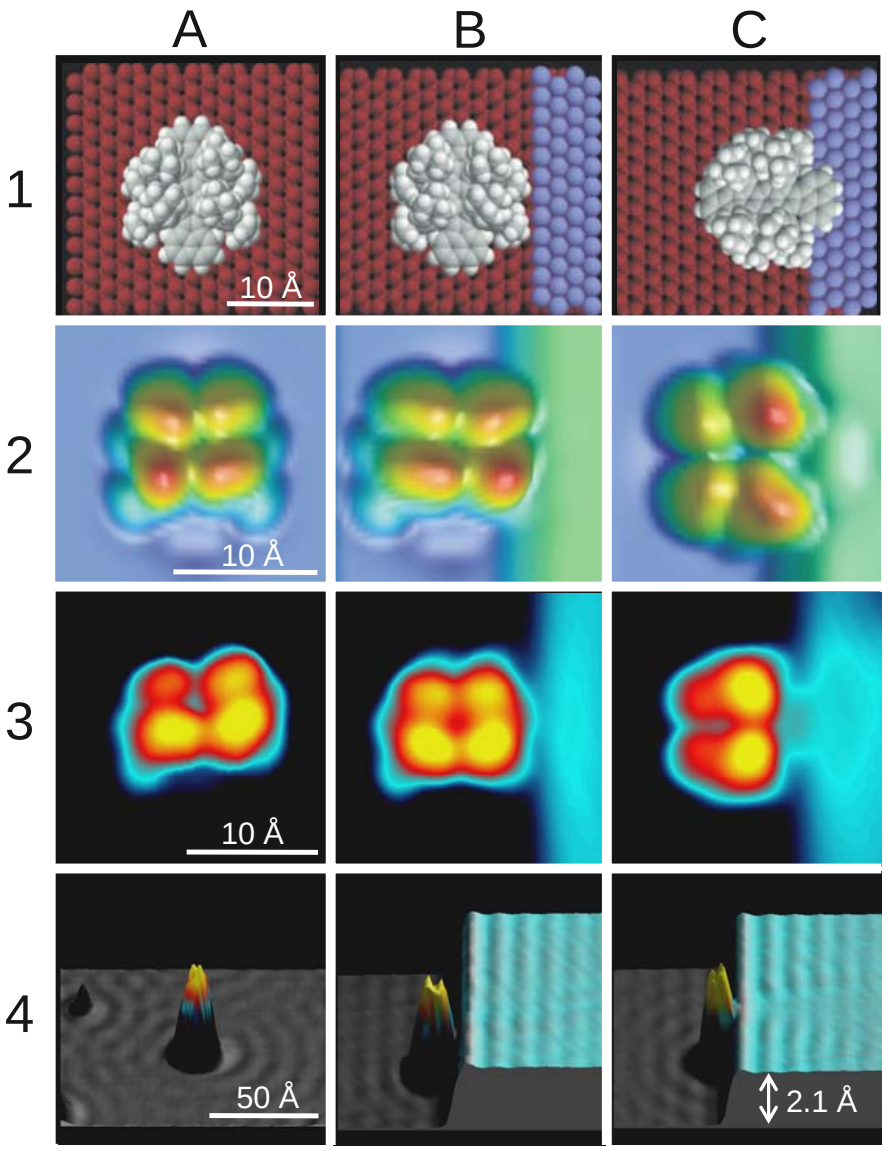

Fig. 5.10. Lander molecules on a free Cu(111) surface (column A) and contacted to a (100) dislocation step. The molecule can be contacted with the molecular board parallel (column B) or orthogonal (column C) to the step. Only in the latter case an influence on the upper terrace becomes visible. In (C2) and (C3) an additional bump corresponding to the contact point of the wire to the step appears and in (C4) a modification of the upper terrace standing wave patterns is visible. Row 1: Ball models of optimised molecular structures. Row 2: Calculated STM images, corresponding to the models above. Row 3: STM measurements. V = 0.8 V, I = 0.2 nA, T = 8 K. Row 4: Pseudo 3-dimensional representation of STM measurements visualizing the standing wave patterns. V = -0.1 V, I = 0.2 nA, T = 8 K.

To bring the wire in contact with a mono atomic step, a chosen Lander that is lying on the lower terrace is laterally manipulated by the STM tip in constant height mode. The tip apex pushes the molecule between two legs, and is forcing it in the direction of the step edge. Knowing the wire orientation relative to the legs, the molecule is pushed towards the step edge with the central wire either parallel or perpendicular to the step. This positioning sequence often requires a tip induced rotation of the molecule, which is performed by using similar conditions like those established for molecular translation. When the legs are within van der Waals distances to the step edge, I stop pushing on the molecule to avoid jumps across the mono-atomic step onto the top terrace. After each re-positioning sequence, the standing wave patterns on the upper terrace are recorded.

When a molecule is pushed to the step with its central wire parallel to it, the Lander reaches the final conformation imaged in Fig. 5.10 B3. The lower CH_3 groups of two lateral legs are at a van der Waals distance to the step (Fig. 5.10 B1) as extracted from the calculated image Fig. 5.10 B2. Separated by the legs, the molecular orbitals of the delocalised electron system of the central wire are not interacting with the step edge. After this manipulation, neither the standing wave patterns on the upper terrace (Fig. 5.10 B4) nor the effect of the molecule on the standing wave patterns on the lower terrace have changed.

The molecule is now re-positioned at the same step with its wire oriented perpendicular to the step edge. A notable modification of the standing wave patterns is observed when the final position of the molecule is reached (Fig. 5.10 C4). The STM-ESQC extraction of the corresponding molecular conformation shows that the terminal naphthalene group of the wire is now on top of the step edge and is electronically weakly coupled with the upper terrace as presented in Fig. 5.10 C1. As a consequence, this naphthalene end is now visible in the STM image of the step edge (Fig. 5.10 C3). This new pattern, hereafter called the contact bump, is located just in between the two front legs as confirmed by calculations (Fig. 5.10 C2). At this stage of the contact sequence, the molecule can be easily de-contacted by a reverse manipulation. This experiment recovers the original step edge and molecule STM images.

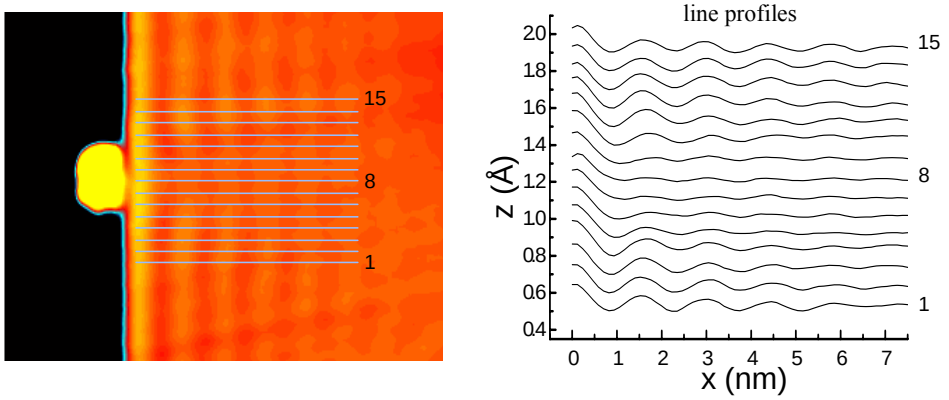

Fig. 5.11. Lander molecule contacted at a step edge (U = -0.1 V, I = 0.2 nA, 14×11 nm²), the line scans correspond to the STM image. The wave amplitude is lowered and the phase is shifted in the region of the contact.

Compared to the clean step edge, the amplitude of the standing wave is reduced at the naphthalene contact location (Fig. 5.10 C4). This effect extends a few 10 nm away from the contact in a characteristic triangular shape. Furthermore a phase shift is also visible in the contact region. Phase shift and damping factor can be quantified, when comparing line scans on the upper terrace, perpendicular to the step edge, as is shown in Fig. 5.12. The line scan at the position of the contact bump (line 8) is damped by a factor of ¼ and the phase is shifted by 26° compared to a line scan at an unperturbed region (line 1 or line 15).

To understand the scattering pattern on the upper terrace I have applied again the formalism of Heller et al.[88] (see section 5.3). The idea is here to vary the size and position of a scatterer near a step edge systematically and correlate the result to the known position and conformation of the molecule. The following model is used to calculate the standing wave pattern: The step edge is modelled by a line of equally spaced black dot scatterers. Their distance of $a_0 = 2.55$ Å corresponds to the distance of atoms in the step edge. To model the molecule a number N of these scatterers is dislocated of the step edge by a distance d (see Fig. 5.12), i.e. I represent the molecule by a series of individual scattering centres, which are in contact with the 2D surface states confined in the upper terrace.

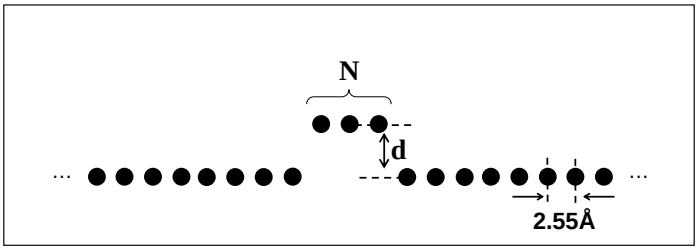

Fig. 5.12. Model used for the calculations of the standing wave patterns. Parameters N and d are used for optimisation. In the case shown: N = 3, d = 4 Å.

To reproduce the experimental STM image, N and d were varied systematically and the wave patterns are calculated and compared with the STM images and line scans. A few calculations near the optimal fit are shown in Fig. 5.13 (varying d at $N = 4$) and Fig. 5.14 (varying N at $d = 2.8$ Å). Electron density patterns have been simulated for ($0 \leq N \leq 10$) and (-10Å $\leq d \leq$ 10Å). Various different geometries also with grey dots have been spot tested and showed less agreement with the experiment.

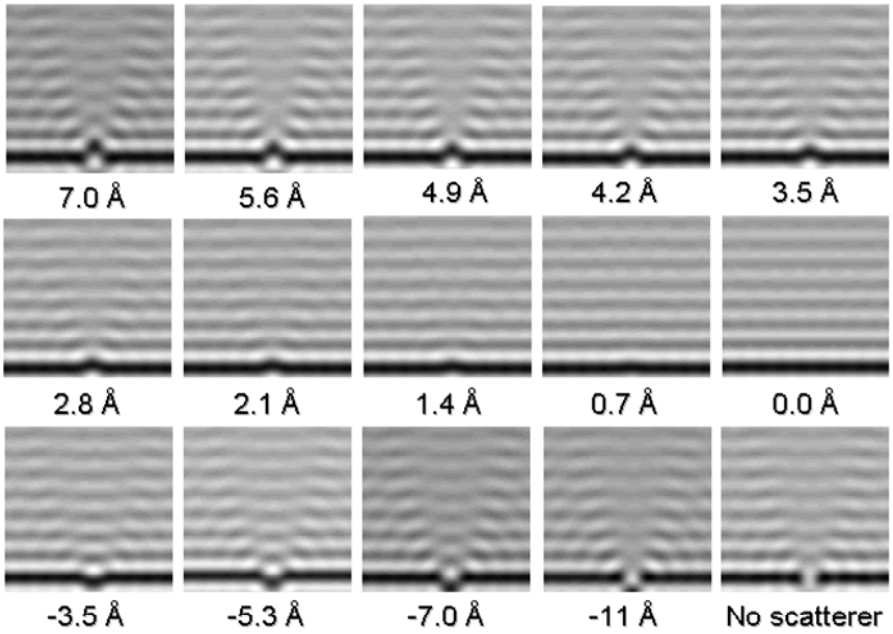

Fig. 5.13. Calculated standing wave patterns for various distances of the scatterers, always $N = 4$, i.e. four scatterers are positioned at the quoted distance off the line of scatterers representing the step edge.

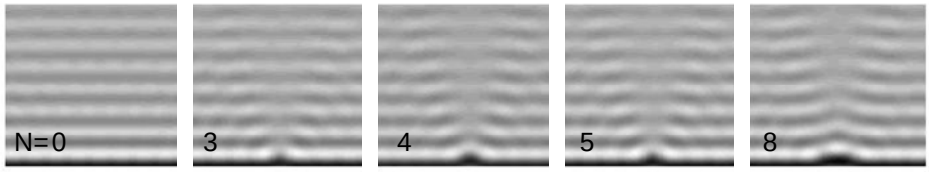

Fig. 5.14. Calculated standing wave patterns for various sizes N of the scatterer, (always with $d = 2.8$) i.e. N black dots are positioned $d = 2.8$ Å off the line of scatterers representing the step edge.

The best agreement between experiment and calculation was realized for $N = 4$ and $d = 0.28$ nm, obtaining the pattern shown in Fig. 5.15(b). The good agreement between STM experiment and numerical simulation indicates that both the formalism and parameterization are good approximations for the experimental system. In particular, this confirms that the π molecular orbitals of the wire interact with the upper terrace surface states through their coupling via the naphthalene end. The naphthalene molecular end acts like an effective 0.76 nm large scatterer which is positioned $d = 0.28$ nm in advance relative to the step edge. This 0.28 nm shift is in agreement with the position of the naphthalene end on the upper terrace as deduced from molecular mechanics calculations (Fig. 5.16). With MM calculations the shift of the naphthalene end onto the upper terrace is estimated as $d_{MM} = 0.23$ nm (Fig. 5.10 C1).[97] The detailed contribution of each π molecular orbital to the scattering process cannot be separated because of the rather large 1.5 nm wavelength of the Cu(111) surface state. The found effective width of 0.76 nm of the scattering centre lies well in the range between the 0.86 nm van der Waals and the 0.63 nm covalent lateral extension of the naphthalene end of the wire.

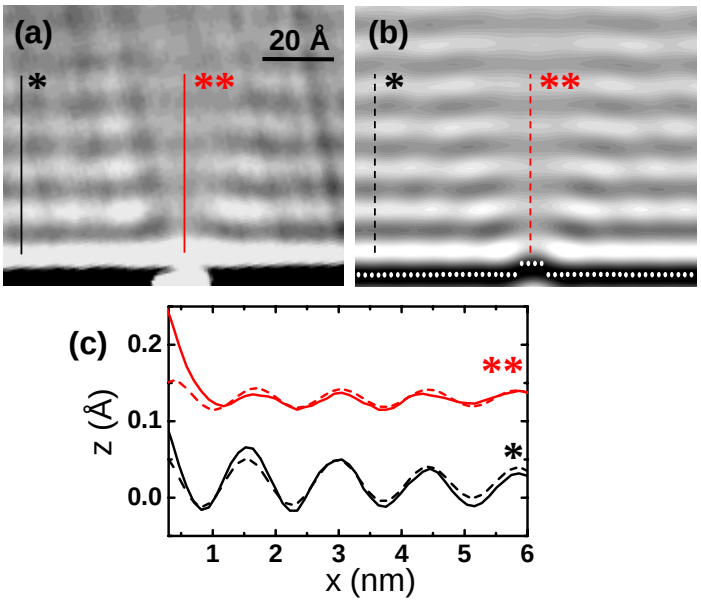

Fig. 5.15. Electron density patterns in the vicinity of a contacted Lander molecule. (a) Measured image, V = -0.1V, I = 0.2 nA, 9x11 nm². (b) Calculated electron density pattern with the best fit, i.e. $N = 4$, $d = 2.8$ Å. Image size 9x11 nm². (c) Line profiles, taken from the measurement (solid lines) and calculation (dashed lines). The height scale of the calculation has been calibrated to the experiment.

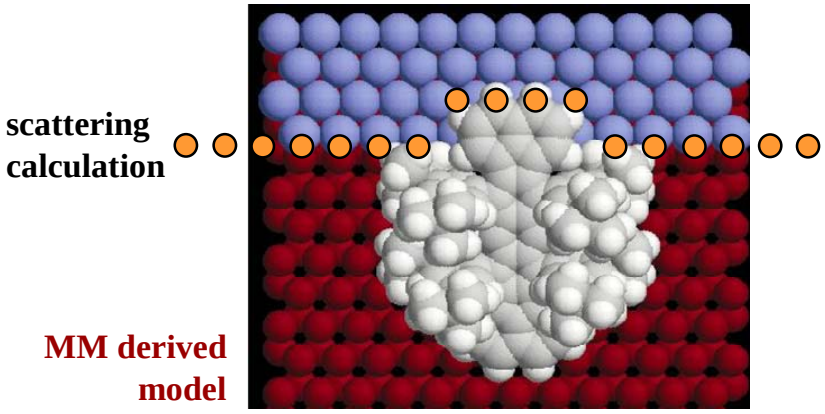

Fig. 5.16. Comparison of the scattering geometry derived by multiple scattering calculations (line of black dot scatterers) and the geometry as derived by the molecular mechanics calculation for the contact position.

The apparent height of the contact bump in the STM image (σ) is an important consequence of the electronic interaction between the naphthalene end and the Cu atoms of the upper terrace. The value for σ has been calculated in the group of C. Joachim[97] in Toulouse as a function of lateral displacement Δx of the molecular board with respect to the step edge. The displacement Δx is defined as the lateral distance between the naphthalene end group of the molecular board and the step edge, with the origin defined as can bee seen in Fig. 5.17. The contact bump height σ is also a function of the vertical distance z between this end and the upper terrace. At the experimental contact position, which corresponds to $\Delta x = +0.48$ nm, the legs constrain the naphthalene end to stay $z = 0.35$ nm above the upper terrace, leading to a calculated $\sigma = 13$ pm to be compared to an experimental value of 15 pm. It is important to note that σ is very small compared to the 100 pm corrugation observed by STM for conjugated molecules chemisorbed on the (111) face of noble metals.[19] This is due to the large height imposed in this case on the naphthalene end by the legs mechanics.

To follow the different stages of the electronic contact, for $z = 0.35$ nm, the variation of σ as a function of Δx without considering the legs (Fig. 5.17, line) has been calculated. The most intense contact bump is expected for Δx around 0.4 nm. For larger positive values of Δx, a larger portion of the wire interacts with the upper terrace. An average value $\sigma = 12.5$ pm is obtained, slightly changing with the relative position of the nodes of the wire molecular orbitals respect to the position of the Cu atoms of the upper terrace. When now the wire is moved sideway from the upper terrace, a σ depression appears in the calculated curve around $\Delta x = 0.2$ nm (Fig. 5.17, dotted line). We attribute it to a lowering of the LDOS at the step edge due to the interaction between the naphthalene end and step edge. For $\Delta x < -0.2$ nm, the mono-atomic step edge recovers its original STM shape and the wire is mechanically and electronically de-contacted.

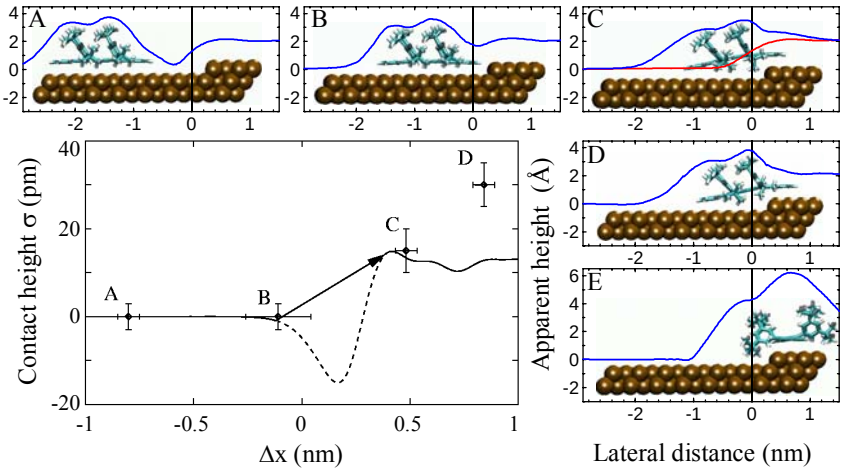

Fig. 5.17. Calculated variation of the contact height σ as a function of the lateral position of the molecular wire relative to the step edge for z = 0.35 nm relative to the upper terrace during the different stages of contacting the end of a Lander molecular wire with a Cu(111) mono-atomic step edge for V_{bias} = 0.8 V. The arrow indicates the actual jump to contact, which overshadows the full exploration of the contact in the depression regime indicated by the dotted line. The 4 experimental points are indicated with their error bars. The experimentally identified conformations A, B, C, D and E are also presented with their corresponding STM experimental scan and the extracted molecular conformation. The experimental scan over an uncovered step edge is provided with the conformation C for comparison together with the Δx origin chosen. Conformation C is corresponds to the contact position as in Fig. 5.10(C). The large apparent contact bump height in D is due to the imaging of the legs CH_3 groups and not of the contact bump itself.

To explore the σ curve experimentally, the molecule has to be manipulated step by step toward the step edge. It is first checked that a molecule is perfectly stable in the conformation A (Fig. 5.17 A) away from the step edge (Δx < -0.2 nm) with σ = 0. For Δx > -0.2 nm, we observe that the molecule is attracted by the step edge towards the mechanical contact conformation B (Fig. 5.17 B). To reach the final electronic contact conformation C (Fig. 5.17 C), the molecule is pushed to pass over a small potential barrier for the naphthalene end to reach the upper terrace. The jump to contact occurs for Δx > 0 nm. As a consequence, a Δx interval of 0.5 nm between B and C is mechanically inaccessible in our case to σ measurements. Occasionally, when pushing again on the molecule, another geometry D (Fig. 5.17 D) of the molecule is observed. Here, the lower CH_3

groups of the front legs have passed over the step edge. In this case, only the depression part of the STM contrast in front of the naphthalene end is imaged because those CH_3 cling to the step, shadowing the contact bump. D is a meta-stable conformation compared to the stable conformation E where the wire is parallel to the step.

The contact experiments and the MM calculations above showed the contacting at a (100), i.e. a A-type step edge. Landers were contacted analogous to (111), i.e. B-type steps, showing equal results.

5.5 Conclusions

The surface state standing wave patterns on Cu(111) created by molecules, which are only weakly interacting with the metallic surface underneath, have been successfully observed. For the first time the scattering wave patterns have been used to probe the molecule-substrate interaction of different molecular parts. To do so, first, the exact molecular adsorption was determined by interplay between STM measurements and MM+ESQC calculations. Then the geometry of point-like scatterers has been optimized in multiple scattering calculations with respect to the experimentally observed patterns, thereby revealing the positions of the chemical groups inside a molecule that are predominant in the scattering process. In particular, I have found that the central molecular wire of Lander type molecules is the predominant scattering site of the molecule. This is an unexpected result since it shows that the molecular board still interacts with the metallic surface, even tough it is elevated from the surface by means of spacer legs. In general, the analysis of electronic standing wave patterns produced by molecules opens a new way to characterize, with a submolecular resolution, the electronic interaction of the molecule with a metallic surface, thus giving insight in the molecule-metal junction, which is not accessible by STM directly.

In the second part of the chapter the contacting of a single molecular wire with its end group to an atomically defined step edge, serving as a contact pad, has been

demonstrated. However, not only this end is connected to the upper terrace, the rest of the molecular board is in electronic interaction with the lower terrace as has been demonstrated before. Although the surface states of upper and lower terrace are largely decoupled by the step edge, the molecular naphthalene end groups are short-circuited by the substrate. Nevertheless, the atomically defined contact of a molecular end to the upper terrace of a single step could be proven and showed exciting new features, i.e. a protrusion due to the contact (contact bump) and characteristic scattering wave patterns of surface state electrons. Due to MM+ESQC and multiple scattering calculations these features could be understood and they could be related to the coupling of the molecular naphthalene end group and the metallic contact pad.

In terms of ongoing research, contact experiments using STM, thereby controlling the exact geometry of the molecule and contact pad are of great importance. The next goal in such experiments can be seen in the performance of I-V measurements of single molecules in dependence on the molecule-metal contact. Therefore the bypassing of the molecular board by the substrate has to be prevented. One possible solution to this problem would be the partial coverage of the surface by insulating or at least semi-conducting adlayers or semi-conducting substrates. In this case contacting experiments could be performed in a similar way as above, but with an insulating layer between molecule and lower terrace. In this scenario no spacer groups for electronic decoupling would be needed. One the other hand further improved molecules could be used. In this case the proper decoupling of a wire part by means of spacer groups could be tested by scattering of surface state electrons as described for the Lander molecules.